

ELSEVIER

Contents lists available at [ScienceDirect](#)

Control Engineering Practice

journal homepage: www.elsevier.com/locate/conengprac



Highlights

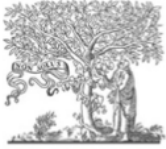
Discrete-time HIGS based digital control of negative imaginary systems

Control Engineering Practice xxx (xxxx) xxx

Kanghong Shi¹, Erfan Khodabakhshi², Prosanto Biswas³, Ian R. Petersen⁴, S. O. Reza Moheimani^{1*}

- A discrete-time hybrid integrator-gain system (HIGS) is a step-advanced negative imaginary (NI) system.
- Motivated by the discrete-time NI systems theory, we prove that discrete-time HIGS can be used to stabilize NI plants.
- This stability result further motivated a digital control methodology for NI plants.
- This digital control methodology is applied to a high-speed flexure-guided nanopositioner in a hardware experiment.

Graphical abstract and Research highlights will be displayed in online search result lists, the online contents list and the online article, but **will not appear in the article PDF file or print unless it is mentioned in the journal specific style requirement. They are displayed in the proof pdf for review purpose only.**

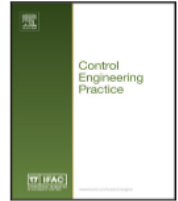


ELSEVIER

Contents lists available at ScienceDirect

Control Engineering Practice

journal homepage: www.elsevier.com/locate/conengprac



Discrete-time HIGS based digital control of negative imaginary systems[☆]

Kanghong Shi^a, Erfan Khodabakhshi^b, Prosanto Biswas^b, Ian R. Petersen^a,
S. O. Reza Moheimani^b,*

^a School of Engineering, College of Systems and Society, Australian National University, Acton, ACT 2601, Australia

^b Erik Jonsson School of Engineering and Computer Science, The University of Texas at Dallas, Richardson, TX 75080, USA

ARTICLE INFO

Keywords:

Negative imaginary system
Hybrid integrator-gain system
Discrete-time system
Digital control
Feedback stability
Switched system
High-speed nanopositioner
Damping control

ABSTRACT

A hybrid integrator-gain system (HIGS) is a control element that switches between an integrator and a gain. This overcomes some inherent limitations of linear controllers. In this paper, we consider using discrete-time HIGS controllers for the digital control of negative imaginary (NI) systems. We show that discrete-time HIGS are step-advanced negative imaginary systems. For a minimal linear NI system, an asymptotically stabilizing HIGS controller always exists. A hardware experiment was carried out in which a flexure-guided nanopositioner, as an example of a linear NI system, was effectively damped using the proposed discrete-time HIGS method.

1. Introduction

Hybrid integrator-gain systems (HIGS) are hybrid control elements, introduced in Deenen et al. (2017), to overcome fundamental limitations of linear time-invariant (LTI) control systems (Freudenberg et al., 2000; Middleton, 1991). A HIGS switches between an integrator mode and a gain mode so that a certain sector constraint is satisfied. To be specific, a HIGS is primarily designed to operate as an integrator, and it switches to the gain mode when its integrator dynamics are about to violate the sector constraint. The describing function of a HIGS has a phase lag of only 38.15 degrees, which is much smaller than the 90 degree phase lag of an integrator. Reset elements including the Clegg integrator (Clegg, 1958) and first-order reset element (Chait & Holot, 2002; Horowitz & Rosenbaum, 1975) also have such advantages. However, they generate discontinuous control signals, which may cause chattering and degrade the system performance (Bartolini, 1989), while the HIGS generates continuous control signals. HIGS controllers have attracted attention since their introduction (e.g., see Deenen et al. (2021), Van den Eijnden et al. (2020, 2023), Heemels and Tanwani (2023), Van Den Eijnden et al. (2021), Dinther et al. (2021)) and have found applications in wafer scanners (Heertjes et al., 2023) and atomic force microscopy (Shi et al., 2022), where the latter work was motivated by the negative imaginary property of HIGS.

Dissipative mechanical systems that feature collocated and compatible force actuators along with position sensors typically demonstrate the negative imaginary (NI) property (Ghallab et al., 2018; Lanzon & Petersen, 2008). Since introduced in Lanzon and Petersen (2008), NI systems theory has attracted significant attention; e.g., see Bhowmick and Patra (2017), Mabrok et al. (2014), Xiong et al. (2010). Motivated by the robust control of flexible structures (Halim & Moheimani, 2001; Pota et al., 2002; Preumont, 2018), which have highly resonant dynamics, NI systems theory uses positive position feedback control. Roughly speaking, a square real-rational proper transfer function matrix $G(s)$ is said to be NI if it has no poles on the open right half-plane and for all frequencies $\omega \geq 0$, its frequency response satisfies $j(G(j\omega) - G(j\omega)^*) \geq 0$. The Nyquist plot of a single-input single-output (SISO) NI system is contained in the lower half of the complex plane. Under mild assumptions, an NI system $G(s)$ can be asymptotically stabilized using a strictly negative imaginary (SNI) system $G_s(s)$ in positive feedback if and only if all the eigenvalues of the DC loop gain matrix are less than unity; i.e., $\lambda_{\max}(G(0)G_s(0)) < 1$. Compared with passivity theory, which can only deal with systems having a relative degree of zero and one (Brogliato et al., 2007), NI systems theory can deal with systems having a relative degree of zero, one or two (Shi et al., 2024d).

[☆] A preliminary version of the present paper Shi and Petersen (2024) has been presented at the 2024 European Control Conference, Stockholm, Sweden. This work was supported by the Australian Research Council under grant DP230102443, and partially by the UTD Center for Atomically Precise Fabrication of Solid-state Quantum Devices.

* Corresponding author.

E-mail addresses: kanghong.shi@outlook.com (K. Shi), erfan@utdallas.edu (E. Khodabakhshi), prosanto.biswas@utdallas.edu (P. Biswas), ian.petersen@anu.edu.au (I.R. Petersen), reza.moheimani@utdallas.edu (S.O.R. Moheimani).

NI systems theory was extended to nonlinear systems in Ghallab et al. (2018), Shi et al. (2023, 2021) via the notion of counterclockwise dynamics (Angeli, 2006). Roughly speaking, a system is said to be nonlinear NI if it is dissipative (Brogliato et al., 2007) with the supply rate $u^T y$. Here, u and y are the input and output of the system, respectively. Under some assumptions, a nonlinear NI system can be stabilized using another nonlinear NI system with a certain strictness property; e.g., output strictly negative imaginary systems (Shi et al., 2023), or weakly strictly negative imaginary systems (Ghallab et al., 2018). NI systems theory has been applied in many fields including nano-positioning control (Das et al., 2014a, 2015; Mabrok et al., 2013), the control of lightly damped structures (Bhikkaji et al., 2011; Cai & Hagen, 2010), and the control of power systems (Chen et al., 2024a, 2024b).

The nonlinear NI property of a HIGS element is shown in Shi et al. (2022). Also, it can be used as a controller to stabilize a linear NI system. Motivated by the effectiveness of HIGS in the control of NI systems, the paper (Shi et al., 2024b) showed the nonlinear NI property of two variants of HIGS, including the multi-HIGS (see also Achten (2020) for a discussion of the multi-HIGS), and the cascade of two HIGS elements. It was also proved in Shi et al. (2024b) that these two variants of HIGS controllers can be used in stabilizing linear NI systems. This HIGS-based control methodology was then experimentally applied to control a MEMS nanopositioner (Shi et al., 2024b).

However, while the stability theory in Shi et al. (2024b) considers continuous-time systems, the experiment involves sampling of the plant outputs and discretization of the controller due to the use of a digital computer (Åström & Wittenmark, 2013). Indeed, in digital control, the continuous-time plant is usually discretized using zero-order hold (ZOH) sampling. The plant outputs are sampled periodically, and the corresponding control inputs are fed back to the plant. The control inputs are held constant between sampling instants. This requires the controller to be a discrete-time system. Therefore, even if the controller is designed in continuous time, it has to be discretized when applied to the plant via a digital controller. The difference between the designed continuous-time controller and the practically implemented discrete-time controller requires the sampling frequency to be sufficiently large to ensure stability (see Nešić et al. (1999) and the references therein for a discussion of the continuous-time design (CTD) method). Such a high sampling frequency may sometimes be unattainable if it exceeds the capability of available control devices. Therefore, we seek to directly design a discrete-time controller.

A discrete-time NI property was introduced in Shi et al. (2024c). It is shown in Shi et al. (2024c) that using this discrete-time NI property, the NI property of a continuous-time NI system is preserved under ZOH sampling. Following Shi et al. (2024c), a discrete-time system is NI if there exists a storage function $V(x)$ such that $V(x)$ is positive definite and $V(x_{k+1}) - V(x_k) \leq u_k^T (y_{k+1} - y_k)$, where x , u and y are the state, input and output of the system, respectively, and the subscripts k and $k + 1$ denote time steps. Considering the storage function as an energy-like function, the above dissipativity inequality corresponds to the work-energy balance relation for a mechanical system: when a constant force is applied to the system, the change in energy over a given time period is not greater than the work done on the system by the applied force. The preservation of the NI property under ZOH sampling can be regarded as an advantage of NI systems theory over passivity or positive real (PR) systems theory, as passivity or positive realness is not preserved under ZOH sampling; see e.g., Brogliato et al. (2007). Note that in Ferrante et al. (2017), a different discrete-time NI property is introduced in a similar fashion as discrete-time passivity (Byrnes & Lin, 1994) and discrete-time positive realness (Hitz & Anderson, 1969). The discrete-time NI property described in Ferrante et al. (2017) can be obtained by applying a bilinear transformation to a continuous-time linear NI system and, hence, does not arise directly in ZOH-sampled NI systems.

A feedback control framework for discrete-time NI systems is given in Shi et al. (2024c). It is shown that the closed-loop interconnection of a discrete-time NI system and a so-called step-advanced negative imaginary (SANI) system is asymptotically stable, as long as either of the systems has some strictness property. Such a digital control framework has motivated the introduction of a linear control system called the discrete-time integral resonant controller in Shi et al. (2024a), for NI plants. In this paper, we consider applying a discrete-time HIGS (Sharif et al., 2022) in such a digital control framework to harness the advantages of HIGS over linear control systems. A discrete-time HIGS has a working mechanism similar to the continuous-time HIGS. We show that a discrete-time HIGS is an SANI system. Furthermore, we establish the following stability result: for any discrete-time NI system: there exists a discrete-time HIGS controller such that their closed-loop interconnection is asymptotically stable.

The NI property and stability results for the HIGS motivate applications for controlling flexible structures with collocated force actuators and position sensors, such as nanopositioning systems. In Shi et al. (2024b), a two-input two-output multi-HIGS controller with positive feedback was implemented on a 2-DOF MEMS nanopositioner. The continuous-time multi-HIGS element was digitally implemented in a dSPACE rapid prototyping system with a sampling rate of 80 kHz. This experiment required discretizing the HIGS controller, an inevitable step when using a digital controller. The plant outputs were periodically sampled and fed back to the discretized HIGS controller, with the corresponding control inputs applied to the plant. Here, the plant inputs were held constant between sampling instants.

Maintaining stability in digital controller implementation heavily depends on the choice of step size. A step size that is too large may lead to instability, while one that is too small may exceed the hardware and computational capability. Also, if the time step is too small, the processing unit may not have adequate time to complete calculations for each step. To avoid degrading system performance, giving the controller adequate processing time within the system's bandwidth constraints is essential.

Additionally, the sampling rate must be large enough for the discretized HIGS controller to represent the designed continuous-time HIGS element accurately. For high-bandwidth nanopositioning systems, minimizing the discrepancy between the designed continuous-time controller and the implemented discrete-time controller necessitates a sufficiently high sampling rate to ensure stability (Nešić et al., 1999), which might not be achievable due to hardware limitations. This motivates the approach presented in this paper to directly design a discrete-time controller.

Motivated by the proposed theoretical results, we apply the discrete-time HIGS based digital control methodology to a high-speed, high-bandwidth nanopositioner. We deployed the HIGS controller within a National Instruments PXIe-7975R FlexRIO module. The digital data was obtained, and the discrete-time controller was operated using an NI-5782 adapter module, which features a 250 MHz clock and allows for a sampling rate of 1.25 MHz.

Compared to the methodology used in Shi et al. (2024b), where the continuous-time HIGS was discretized and implemented, using a discrete-time HIGS has the following two advantages: (i) It can significantly simplify the control design process. We directly construct a discrete-time controller for the discretized plant, while the methodology used in Shi et al. (2024b) requires further discretization for the continuous-time controller. This can help decrease time delay and save computational resources. (ii) As we conduct the stability analysis directly in discrete time, the stability result is more rigorous and does not rely on a high sampling rate.

The rest of the paper is organized as follows. Section 2 provides preliminary definitions and lemmas for discrete-time NI systems that are introduced in Shi et al. (2024c). Section 2 also provides the state-space model of a discrete-time HIGS. Section 3 contains the theoretical

results of this paper, where we establish the NI property of the discrete-time HIGS. We also show that given a linear discrete-time NI plant, there always exists a HIGS controller that can stabilize the system. In Section 4, we apply the proposed digital control methodology to the nanopositioning system. Also presented in Section 4 are the experimental setup, the frequency response of the nanopositioner, the discrete-time HIGS controller implementation, and the experimental results. Section 5 concludes the paper and discusses potential future work. A preliminary version of this article can be found in the conference paper (Shi & Petersen, 2024). In comparison with the preliminary version (Shi & Petersen, 2024), the present paper applies the proposed HIGS control methodology in a hardware experiment to control a high-speed flexure-guided nanopositioner. Also, the introduction of the present article includes a more detailed explanation of the problem addressed and the contributions of our results.

Notation: The notation in this paper is standard. \mathbb{R} denotes the field of real numbers. \mathbb{N} denotes the set of nonnegative integers. $\mathbb{R}^{m \times n}$ denotes the space of real matrices of dimension $m \times n$. A^T denotes the transpose of a matrix A . A^{-T} denotes the transpose of the inverse of A ; that is, $A^{-T} = (A^{-1})^T = (A^T)^{-1}$. For a real symmetric or complex Hermitian matrix P , $P > 0$ ($P \geq 0$) denotes the positive (semi-)definiteness of the matrix P and $P < 0$ ($P \leq 0$) denotes the negative (semi-)definiteness of the matrix P . A function $V : \mathbb{R}^n \rightarrow \mathbb{R}$ is said to be positive definite if $V(0) = 0$ and $V(x) > 0$ for all $x \neq 0$. $\lambda_{\max}(A)$ denotes the largest eigenvalue of a matrix A with real spectrum.

2. Preliminaries

In this section, we provide some preliminary results on discrete-time NI systems and discrete-time HIGS.

2.1. Discrete-time NI systems

Consider the system

$$x_{k+1} = f(x_k, u_k), \quad (1a)$$

$$y_k = h(x_k), \quad (1b)$$

where $f : \mathbb{R}^n \times \mathbb{R}^p \rightarrow \mathbb{R}^n$ and $h : \mathbb{R}^n \rightarrow \mathbb{R}^p$. Here $u_k, y_k \in \mathbb{R}^p$ and $x_k \in \mathbb{R}^n$ are the input, output and state of the system at time step $k \in \mathbb{N}$, respectively.

Definition 1 (Shi et al., 2024c). The system (1) is said to be a discrete-time negative imaginary (NI) system if there exists a positive definite function $V : \mathbb{R}^n \rightarrow \mathbb{R}$ such that for arbitrary x_k and u_k ,

$$V(x_{k+1}) - V(x_k) \leq u_k^T (y_{k+1} - y_k), \quad (2)$$

for all k .

We provide necessary and sufficient linear matrix inequality (LMI) conditions under which Definition 1 is satisfied by a linear system of the form

$$\Sigma : x_{k+1} = Ax_k + Bu_k, \quad (3a)$$

$$y_k = Cx_k, \quad (3b)$$

where $x_k \in \mathbb{R}^n$, $u_k, y_k \in \mathbb{R}^p$ are the system state, input and output, respectively.

Lemma 1 (Shi et al., 2024c). Suppose the linear system (3) satisfies $\det(I - A) \neq 0$. Then the system (3) is NI with a positive definite quadratic storage function satisfying (2) if and only if there exists a real matrix $P = P^T > 0$ such that

$$A^T P A - P \leq 0 \quad \text{and} \quad C = B^T (I - A)^{-T} P.$$

We now present the definition of SANI systems. Consider the system

$$\tilde{x}_{k+1} = \tilde{f}(\tilde{x}_k, \tilde{u}_k), \quad (4a)$$

$$\tilde{y}_k = \tilde{h}(\tilde{x}_k, \tilde{u}_k), \quad (4b)$$

where $\tilde{f} : \mathbb{R}^n \times \mathbb{R}^p \rightarrow \mathbb{R}^n$ and $\tilde{h} : \mathbb{R}^n \rightarrow \mathbb{R}^p$. Here $\tilde{u}, \hat{y} \in \mathbb{R}^p$ and $\tilde{x} \in \mathbb{R}^n$ are the input, output and state of the system at time step $k \in \mathbb{N}$, respectively.

Definition 2 (Shi et al., 2024c). The system (4) is said to be a step-advanced negative imaginary (SANI) system if there exists a function $\tilde{h}(\tilde{x}_k)$ such that:

1. $\tilde{h}(\tilde{x}_k, \tilde{u}_k) = \hat{h}(\tilde{f}(\tilde{x}_k, \tilde{u}_k))$;
2. there exists a positive definite function $\tilde{V} : \mathbb{R}^n \rightarrow \mathbb{R}$ such that for arbitrary state \tilde{x}_k and input \tilde{u}_k ,

$$\tilde{V}(\tilde{x}_{k+1}) - \tilde{V}(\tilde{x}_k) \leq \tilde{u}_k^T \left(\hat{h}(\tilde{x}_{k+1}) - \hat{h}(\tilde{x}_k) \right)$$

for all k .

Remark 1. Definition 2 can be regarded as a variant of Definition 1 in a way such that the system output takes one step advance. To be specific, suppose the system (1) is NI as per Definition 1. Then a system with the same state Eq. (1a) and an output equation $\tilde{y}_k = h(x_{k+1}) = h(f(x_k, u_k))$ is SANI. Note this system is causal, given that $h(f(x_k, u_k))$ depends only on the system variables of the current step.

2.2. Discrete-time hybrid integrator-gain systems

Discrete-time HIGS were introduced in Sharif et al. (2022). We adapt the model in Sharif et al. (2022) to fit the system model (1) in the following.

$$\mathcal{H} : \begin{cases} x_h(k+1) = x_h(k) + \omega_h e(k), & \text{if } (x_h(k), e(k)) \in \mathcal{F} \\ x_h(k+1) = k_h e(k), & \text{if } (x_h(k), e(k)) \notin \mathcal{F} \\ y_h(k) = x_h(k+1). \end{cases} \quad (5)$$

Here, $e(k), x_h(k), y_h(k) \in \mathbb{R}$ are the system input, state and output, respectively. The constant parameters $\omega_h \geq 0$ and $k_h > 0$ are called the integrator frequency and the gain value, respectively. The HIGS is designed to operate under the sector constraint $(x_h(k), e(k)) \in \mathcal{F}$, where \mathcal{F} is given by

$$\mathcal{F} = \{(x_h(k), e(k)) \in \mathbb{R}^2 \mid (x_h(k) + \omega_h e(k))e(k) \geq \frac{1}{k_h} (x_h(k) + \omega_h e(k))^2\}. \quad (6)$$

At time step k , if $(x_h(k), e(k)) \in \mathcal{F}$, then $(e(k), y_h(k))$ is contained in the sector $[0, k_h]$. The HIGS is designed to operate primarily in the integrator mode if the input $e(k)$ results in an output $y_h(k)$ within the sector $[0, k_h]$ under the integrator mode dynamics. Otherwise, the system operates in the gain mode so that $y_h(k) = k_h e(k)$, which automatically satisfies the sector constraint $[0, k_h]$. According to (5), regardless of the initial condition $x_h(0)$, the discrete-time HIGS will remain in the sector given in \mathcal{F} from the time step $k = 1$. In what follows, we denote $e(k), x_h(k)$ and $y_h(k)$ by e_k, \tilde{x}_k and \tilde{y}_k respectively for convenience. Note that the parameter ω_h in the present paper corresponds to the product $\omega_h T_s$ in Sharif et al. (2022), where ω_h is the integrator frequency of the corresponding continuous-time integrator and T_s is the sampling period. Since we only consider the discrete-time case in the present paper, we regard ω_h as the discrete-time integrator frequency.

3. Stability of NI systems under discrete-time HIGS control

In this section, we show that a discrete-time HIGS is an SANI system according to Definition 2. Additionally, we show that for a discrete-time linear NI system, there exists a discrete-time HIGS such that their closed-loop interconnection is asymptotically stable. Sufficient conditions on the HIGS parameters are also given.

3.1. SANI property of the HIGS

We show in the following that the HIGS given in (5) is an SANI system.

Theorem 1. *The system given in (5) is an SANI system with the storage function*

$$\tilde{V}(\tilde{x}_k) = \frac{1}{2k_h} \tilde{x}_k^2 \quad (7)$$

satisfying

$$\tilde{V}(\tilde{x}_{k+1}) - \tilde{V}(\tilde{x}_k) \leq e_k(\tilde{x}_{k+1} - \tilde{x}_k), \quad (8)$$

for any input e_k and state \tilde{x}_k .

Proof. According to Definition 2 and Remark 1, the HIGS is an SANI system if it is NI from the input e_k to the state \tilde{x}_k . Hence, we prove in the following that (8) is satisfied in both integrator mode and gain mode. Substituting (7) into (8) yields

$$\frac{1}{2k_h} \tilde{x}_{k+1}^2 - \frac{1}{2k_h} \tilde{x}_k^2 \leq e_k(\tilde{x}_{k+1} - \tilde{x}_k), \quad (9)$$

which is required to be satisfied in both modes.

Case 1. In the integrator mode, we have the state equation $\tilde{x}_{k+1} = \tilde{x}_k + \omega_h e_k$ and also $(\tilde{x}_k, e_k) \in \mathcal{F}$. In this case, (9) becomes

$$2\tilde{x}_k e_k \leq (2k_h - \omega_h) e_k^2, \quad (10)$$

which is always satisfied when $e_k = 0$. When $e_k \neq 0$, (10) can be rewritten as

$$2 \frac{\tilde{x}_k}{e_k} \leq 2k_h - \omega_h. \quad (11)$$

The condition $(\tilde{x}_k, e_k) \in \mathcal{F}$ implies

$$\tilde{x}_k^2 + (2\omega_h - k_h)\tilde{x}_k e_k + (\omega_h - k_h\omega_h)e_k^2 \leq 0.$$

This implies that for $e_k \neq 0$,

$$\left(\frac{\tilde{x}_k}{e_k}\right)^2 + (2\omega_h - k_h)\frac{\tilde{x}_k}{e_k} + (\omega_h^2 - k_h\omega_h) \leq 0. \quad (12)$$

By solving (12), we have that operating in the integrator mode requires the HIGS input e_k and state \tilde{x}_k to satisfy

$$-\omega_h \leq \frac{\tilde{x}_k}{e_k} \leq k_h - \omega_h.$$

Such a pair of \tilde{x}_k and e_k always satisfies (11).

Case 2. In the gain mode, we have that $\tilde{x}_{k+1} = k_h e_k$ and $(\tilde{x}_k, e_k) \notin \mathcal{F}$. In this case, (9) becomes

$$\tilde{x}_k^2 - 2k_h \tilde{x}_k e_k + k_h^2 e_k^2 \geq 0,$$

which always holds because

$$\tilde{x}_k^2 - 2k_h \tilde{x}_k e_k + k_h^2 e_k^2 = (\tilde{x}_k - k_h e_k)^2 \geq 0.$$

Since condition (8) is satisfied in both modes, we may conclude that the system (5) is an SANI system. ■

3.2. Stability for the interconnection of a linear NI system and a HIGS

Motivated by the SANI property of the HIGS, we investigate whether a HIGS controller can be applied to control a minimal SISO linear NI system. Consider a SISO system of the form (3) with $u_k, y_k \in \mathbb{R}$, which has a transfer function $G(z)$. We show in the following that if the system Σ in (3) is NI, then there exists a HIGS controller \mathcal{H} such that the positive feedback interconnection of Σ and \mathcal{H} , shown in Fig. 1, is asymptotically stable. The setting of the interconnection can be described as follows:

$$e_k = y_k;$$

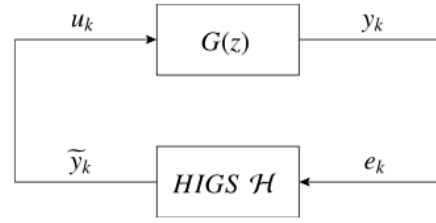


Fig. 1. Closed-loop interconnection of the system (3) with the transfer function $G(z)$ and the HIGS \mathcal{H} given in (5).

$$u_k = \tilde{y}_k.$$

This means the HIGS \mathcal{H} takes the output of the system Σ as its input and feeds back its output to the system Σ as its input.

Theorem 2. *Suppose the SISO minimal system (3) with transfer function $G(z)$ is NI and satisfies $\det(I - A) \neq 0$. Also, suppose the HIGS \mathcal{H} of the form (5) satisfies $0 < \omega_h \leq k_h < \frac{1}{G(1)}$. Then, the closed-loop interconnection of $G(z)$ and \mathcal{H} as shown in Fig. 1 is asymptotically stable.*

Proof. By Lemma 1, the minimal system (3) is NI if and only if there exists a matrix $P = P^T > 0$ such that

$$A^T P A - P \leq 0, \text{ and } C = B^T (I - A)^{-T} P.$$

We construct the following Lyapunov function for the closed-loop interconnection:

$$\begin{aligned} W(x_k, \tilde{x}_k) &= V(x_k) + \tilde{V}(\tilde{x}_k) - C x_k \tilde{x}_k \\ &= \frac{1}{2} x_k^T P x_k + \frac{1}{2k_h} \tilde{x}_k^2 - C x_k \tilde{x}_k. \end{aligned}$$

Rewriting this as a quadratic form, we have that

$$W(x_k, \tilde{x}_k) = \frac{1}{2} \begin{bmatrix} x_k^T & \tilde{x}_k \end{bmatrix} \begin{bmatrix} P & -C^T \\ -C & \frac{1}{k_h} \end{bmatrix} \begin{bmatrix} x_k \\ \tilde{x}_k \end{bmatrix}.$$

Using the Schur complement theorem, to ensure that $W(x_k, \tilde{x}_k)$ is positive definite, we need

$$\frac{1}{k_h} - C P^{-1} C^T > 0. \quad (13)$$

Since $C = B^T (I - A)^{-T} P$, then (13) can be rewritten as

$$\frac{1}{k_h} - C(I - A)^{-1} B > 0,$$

which is satisfied because $G(1) = C(I - A)^{-1} B$ and

$$k_h G(1) < 1. \quad (14)$$

Note that $G(1) \neq 0$ according to the positive definiteness of P and the fact that C is not a zero row vector, which is guaranteed by the minimality of the system. We use Lyapunov's direct method (Kalman & Bertram, 1960) in the following. Taking the difference between $W(x_{k+1}, \tilde{x}_{k+1})$ and $W(x_k, \tilde{x}_k)$, we have

$$\begin{aligned} &W(x_{k+1}, \tilde{x}_{k+1}) - W(x_k, \tilde{x}_k) \\ &= V(x_{k+1}) + \tilde{V}(\tilde{x}_{k+1}) - C x_{k+1} \tilde{x}_{k+1} - V(x_k) - \tilde{V}(\tilde{x}_k) + C x_k \tilde{x}_k \\ &\leq u_k (y_{k+1} - y_k) + e_k (\tilde{x}_{k+1} - \tilde{x}_k) - C x_{k+1} \tilde{x}_{k+1} + C x_k \tilde{x}_k \\ &= \tilde{x}_{k+1} (e_{k+1} - e_k) + e_k (\tilde{x}_{k+1} - \tilde{x}_k) - e_{k+1} \tilde{x}_{k+1} + e_k \tilde{x}_k \\ &= 0, \end{aligned} \quad (15)$$

where the inequality also uses the NI properties of the plant $G(z)$ and the HIGS controller \mathcal{H} . This implies that the system is Lyapunov stable. Furthermore, according to (15), $W(x_{k+1}, \tilde{x}_{k+1}) - W(x_k, \tilde{x}_k) = 0$ only if the following equations hold:

$$V(x_{k+1}) - V(x_k) = u_k (y_{k+1} - y_k); \quad (16)$$

$$\tilde{V}(\tilde{x}_{k+1}) - \tilde{V}(\tilde{x}_k) = e_k(\tilde{x}_{k+1} - \tilde{x}_k). \quad (17)$$

We prove in the following that (16) and (17) cannot hold together at all time indices k unless $(x_k, \tilde{x}_k) = (0, 0)$. We consider the case that (16) and (17) hold for some index k and all future indices $k+1, k+2, \dots$. When (17) holds, we have that

$$\frac{1}{2k_h} \tilde{x}_{k+1}^2 - \frac{1}{2k_h} \tilde{x}_k^2 = e_k(\tilde{x}_{k+1} - \tilde{x}_k). \quad (18)$$

We consider the following two cases, where the HIGS is assumed to work in the integrator mode and the gain mode, respectively.

Case 1. Integrator mode. In this case, $(\tilde{x}_k, e_k) \in \mathcal{F}$ and

$$\tilde{x}_{k+1} = \tilde{x}_k + \omega_h e_k. \quad (19)$$

Substituting (19) in (18) yields

$$(\omega_h - 2k_h)e_k^2 + 2\tilde{x}_k e_k = 0. \quad (20)$$

Case 1a. Suppose $e_k \neq 0$. Then we have $\tilde{x}_k = (k_h - \frac{\omega_h}{2})e_k$, which can be substituted in the inequality in (6) and yields

$$(k_h + \frac{\omega_h}{2})e_k^2 \geq \frac{1}{k_h}(k_h + \frac{\omega_h}{2})^2 e_k^2.$$

This, after simplification, becomes

$$\omega_h^2 + 2k_h\omega_h \leq 0.$$

Considering the fact that $k_h > 0$ and $\omega > 0$, the above condition can never be satisfied. Hence, *Case 1a* can never happen.

Case 1b. Suppose $e_k = 0$. Then (20) is always satisfied. In this case, $(\tilde{x}_k, e_k) \in \mathcal{F}$ implies that $\tilde{x}_k = 0$. According to (19), we have that $\tilde{x}_{k+1} = 0$ as well. The condition for $(\tilde{x}_{k+1}, e_{k+1}) \in \mathcal{F}$ can be simplified to be

$$(k_h - \omega_h)e_{k+1}^2 \geq 0.$$

The fact that $k_h - \omega_h \geq 0$ guarantees that the next active mode is the integrator mode. Note that this condition is independent of the HIGS input or state. Indeed, since *Case 1a* can never happen, the system will fall in *Case 1b* for all future time indices $k+1, k+2, \dots$. Following from a similar analysis, we have that

$$0 = e_k = e_{k+1} = e_{k+2} = \dots, \quad (21)$$

and also

$$0 = \tilde{x}_k = \tilde{x}_{k+1} = \tilde{x}_{k+2} = \dots. \quad (22)$$

Since $u_k = \tilde{y}_k = \tilde{x}_{k+1}$, then according to (22) and (3a), we have that

$$x_{k+1} = Ax_k, \quad x_{k+2} = Ax_{k+1} = A^2x_k, \quad \dots \quad (23)$$

Since $e_k = y_k = Cx_k$, then according to (21) and (23), we have that

$$\begin{bmatrix} C \\ CA \\ \vdots \\ CA^{n-1} \end{bmatrix} x_k = 0.$$

This implies that $x_k = 0$ due to the observability of $G(z)$. In this case, $(x_k, \tilde{x}_k) = (0, 0)$. Hence, the closed-loop system is already in its equilibrium.

Case 2. Gain mode. In this case, $(\tilde{x}_k, e_k) \notin \mathcal{F}$, and we have that

$$\tilde{x}_{k+1} = k_h e_k. \quad (24)$$

Substituting (24) in (18), we have that

$$(\tilde{x}_k - k_h e_k)^2 = 0.$$

That is

$$\tilde{x}_k = k_h e_k = \tilde{x}_{k+1}. \quad (25)$$

The condition $(\tilde{x}_k, e_k) \notin \mathcal{F}$ implies that

$$(k_h + \omega_h)e_k^2 > 0.$$

This implies that $e_k \neq 0$. We only need consider the case that the HIGS operates in the gain mode for all future indices. This is because under the constraints (17), if it enters the integrator mode, it will never exit the integrator mode, according to the analysis in *Case 1b*. Then it falls into *Case 1*. In the case that the system keeps operating in the gain mode, following from the same derivation of (25), we have that

$$\tilde{x}_{k+1} = k_h e_{k+1} = \tilde{x}_{k+2}. \quad (26)$$

Comparing (25), (26) and similar equations for future time indices, we have that

$$\tilde{x}_k = k_h e_k = \tilde{x}_{k+1} = k_h e_{k+1} = \tilde{x}_{k+2} = k_h e_{k+2} = \dots.$$

That is

$$e_k = e_{k+1} = e_{k+2} = \dots.$$

This implies that

$$y_k = y_{k+1} = y_{k+2} = \dots. \quad (27)$$

In this case, we have that

$$\begin{aligned} x_{k+1} &= Ax_k + Bu_k = Ax_k + B\tilde{y}_k = Ax_k + B\tilde{x}_{k+1} \\ &= Ax_k + Bk_h e_k = Ax_k + k_h BCx_k \\ &= (A + k_h BC)x_k. \end{aligned}$$

Similarly, we have

$$\begin{aligned} x_{k+2} &= (A + k_h BC)x_{k+1} = (A + k_h BC)^2 x_k, \\ &\vdots \\ x_{k+n-1} &= (A + k_h BC)^{n-1} x_k. \end{aligned}$$

According to (27), we have that

$$\begin{bmatrix} y_{k+1} - y_k \\ y_{k+2} - y_{k+1} \\ \vdots \\ y_{k+n} - y_{k+n-1} \end{bmatrix} = 0,$$

which implies

$$\begin{bmatrix} C \\ C(A + k_h BC) \\ \vdots \\ C(A + k_h BC)^{n-1} \end{bmatrix} (x_{k+1} - x_k) = 0. \quad (28)$$

We use eigenvector test to prove that observability of (A, C) implies that of $(A + k_h BC, C)$. Suppose $\eta \neq 0$ is a vector in the kernel of C ; i.e., $C\eta = 0$. Then it is not an eigenvector of A ; i.e., $A\eta \neq \lambda\eta$ for all scalars λ . Then η is not an eigenvector of $A + k_h BC$ as well because $(A + k_h BC)\eta = A\eta + k_h BC\eta = A\eta \neq \lambda\eta$ for all λ , considering $C\eta = 0$. Hence, $(A + k_h BC, C)$ is observable and (28) implies that $x_{k+1} = x_k$. That is, x_k is an eigenvector of $A + k_h BC$ with an eigenvalue $\lambda = 1$. This implies that

$$x_k = x_{k+1} = x_{k+2} = \dots.$$

In this case, we also have that

$$\begin{aligned} x_k &= x_{k+1} = Ax_k + Bu_k = Ax_k + B\tilde{y}_k = Ax_k + B\tilde{x}_{k+1} \\ &= Ax_k + Bk_h e_k. \end{aligned}$$

This implies that

$$x_k = k_h(I - A)^{-1}Be_k.$$

Also, we have that

$$e_k = Cx_k = k_h C(I - A)^{-1}Be_k. \quad (29)$$

Since we have $e_k \neq 0$ in *Case 2*, then (29) implies that

$$k_h C(I - A)^{-1}B = 1,$$

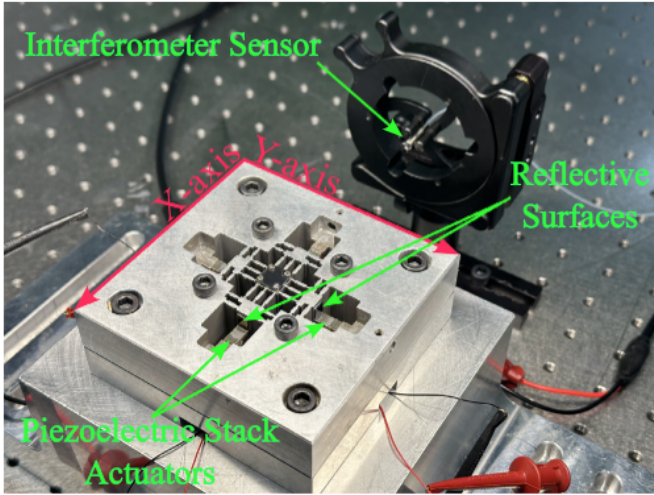


Fig. 2. Flexure-guided nanopositioner and interferometer sensor.

which is

$$k_h G(1) = 1.$$

This contradicts (14). To conclude, we have shown that if (16) and (17) hold together for all future time indices, then the HIGS cannot stay in the gain mode according to the analysis in *Case 2*. It will eventually switch to the integrator mode. Then, according to the analysis in *Case 1*, the HIGS will stay in the integrator mode. However, we have shown in *Case 1b* that this is only possible if the system is already at the equilibrium. In other words, if the system is not at the equilibrium, then (16) and (17) cannot hold together for all future indices, and $W(x_k, \tilde{x}_k)$ will eventually decrease again until the system reaches its equilibrium. This means that the closed-loop system is asymptotically stable. ■

4. Experiment: High-speed flexure-guided nanopositioner

We implement a discrete-time HIGS as a controller for a high-speed flexure-guided nanopositioning stage, which is configured as a linear NI system.

Fig. 2 illustrates the experimental setup for the high-speed flexure-guided nanopositioner introduced in Khodabakhshi et al. (2022). Four piezoelectric actuators drive the nanopositioner in a bidirectional actuation setup. A PICOSCALE interferometer achieves high-precision measurements in the X - and Y - directions. Fig. 3 presents the frequency response function (FRF) of the X -axis nanopositioner, showing the system's behavior from actuation to the sensor output. A lightly damped nanopositioning system with collocated and compatible force actuators and position sensors is an NI system by its physical nature. In Fig. 3, the fundamental resonance frequency along the X -axis is observed at 14.86 kHz. Beyond 15.01 kHz, the phase drops below -180° , indicating a violation of the NI property as the frequency increases. This deviation comes from the driving electronics' bandwidth limitations and fabrication tolerances, as well as sampling and input-output delays. However, this phase deviation is negligible as the frequency response rolls off. Therefore, we can still approximate the system using an NI model up to a certain frequency. The following sections will describe the implementation of the designed discrete-time HIGS.

4.1. Experimental setup

Fig. 4 depicts the experimental setup. The displacement of the scanner is measured using a highly accurate optical sensor called a Michelson interferometer. The sensor measurements are recorded as Digital Differential Interface (DDI) signals through the PICOSCALE

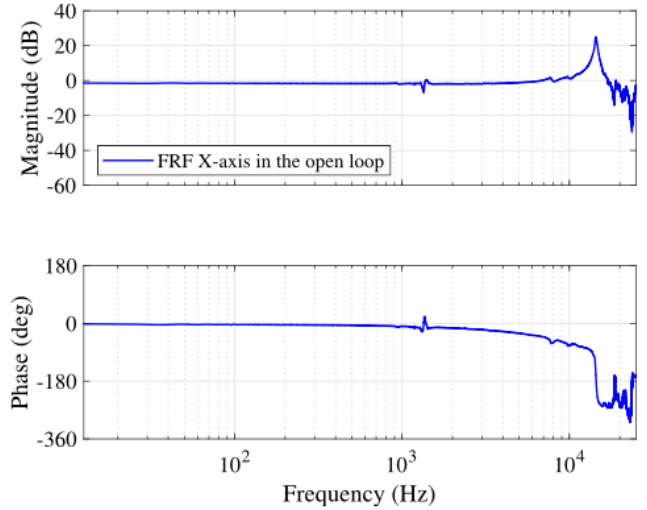


Fig. 3. Open-loop frequency response of the nanopositioner.

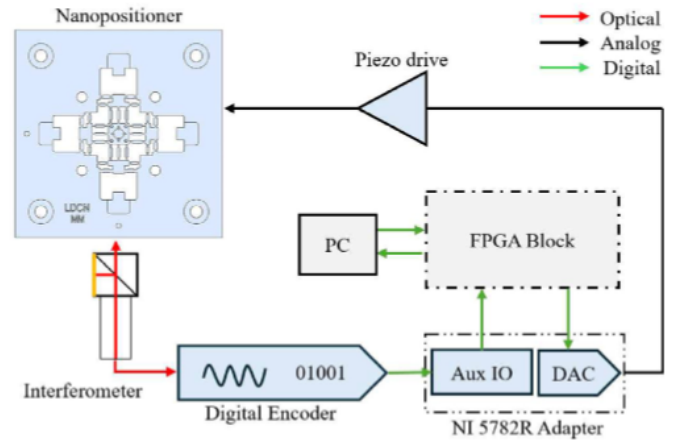


Fig. 4. Experimental setup FPGA.

Breakout Box (BOB). The recorded DDI signals, formatted as Quadrature (AquadB), are then fine-tuned to achieve the required resolution in terms of step size and frequency. A quadrature decoder is then implemented within the LabVIEW FPGA environment to convert these signals into position values in micrometers, along with the discrete-time HIGS.

The quadrature decoder operates using the encoder's two phases, Quad A and Quad B, which have an offset of 90° . The current state of Quad B is compared with the previous state of Quad A so that the count is adjusted accordingly. An initial reset circuit setup is necessary since PICOSCALE tracks only relative displacement. Each count is multiplied by a factor corresponding to the 6 nm step size, based on experimental results showing sensor noise below 6 nm.

4.2. FPGA implementation

Our primary processor is a Kintex-7 XC7K410T FPGA within a National Instruments PXIe-7975R FlexRIO module. It connects to a National Instruments 5782R adapter, which is a 14-bit, four-channel digitizer with a 500 MHz bandwidth and a 250 MS/s sampling rate. FPGA development is done in the LabVIEW FPGA environment.

We programmed the above components within a single-cycle timed loop (SCTL). This can optimize performance and also reduce latency. A voltage converter adjusts the DDI output to match the adapter's input voltage. The decoder, operating at 250 MHz, rapidly converts digital data to position parameters. However, due to the complexity of the

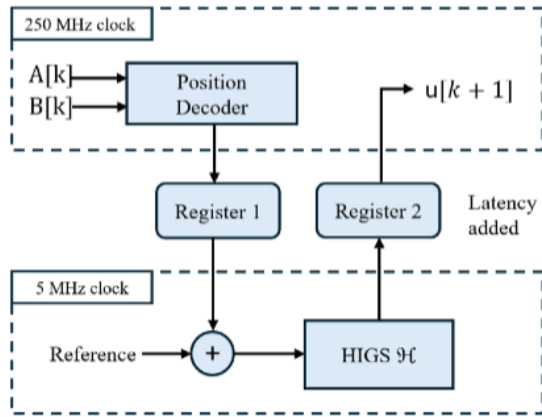


Fig. 5. FPGA workflow of a discrete-time HIGS at 1.25 MHz sampling rate.

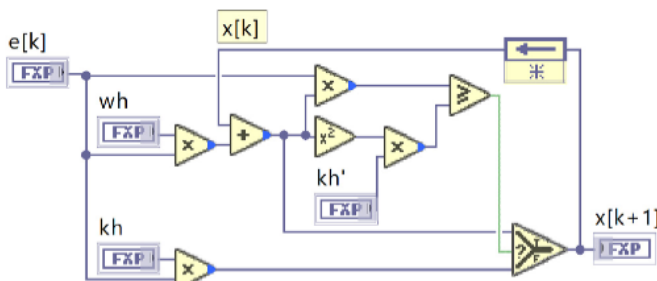


Fig. 6. Discrete-time HIGS implemented in the labVIEW FPGA.

discrete-time HIGS operations, which exceed the 4 ns cycle limit, data is transferred to a slower 5 MHz SCTL derived from the 250 MHz oscillator (see Fig. 5). Due to the buffer latency, the effective sampling rate is decreased to 1.25 MHz.

Fig. 6 shows the digital implementation of the discrete-time HIGS (5) in the LabVIEW environment. Integer-type variables are used in the high-frequency loop for faster processing, while fixed-point data formats in the slower loop offer customizable range and resolution. Inside the implemented discrete-time HIGS block, a new variable $k'_h = \frac{1}{k_h}$ is defined as a multiplier since division is not supported within SCTL. Observation shows that the discrete-time HIGS is more efficient than the continuous-time version, requiring less memory and processing power, thus reducing latency.

Theorem 2 indicates that the nanopositioner can be asymptotically stabilized using the discrete-time HIGS (5) if the HIGS parameters satisfy $0 < \omega_h \leq k_h < 1/G(1)$. We tuned the controller parameters to meet the stability condition and to obtain performance improvement as desired. Accordingly, the parameter values $\omega_h = 0.0704$ and $k_h = 0.490$ are chosen for the discrete-time HIGS.

Fig. 7 presents the frequency response of the nanopositioning stage when operating in the closed loop with the discrete-time HIGS. The results show that significant damping, approximately 20.4 dB, is obtained at the resonance frequency.

We also compared the time-domain response of the open-loop and the closed-loop system to a unit step in Fig. 8. The reason that stability can be achieved although the plant is only NI up to 15.01 kHz is that the magnitude of the frequency response of the nanopositioner is bounded below a certain level when the frequency is greater than 15.01 kHz. In this case, the stability is achieved via the small-gain theorem; see Das et al. (2014b), Patra and Lanzon (2011) for the stability of systems with “mixed” NI and small-gain properties. Fig. 8 also shows significant improvements in the system performance under the control of the discrete-time HIGS, including reduced overshoot and settling time.

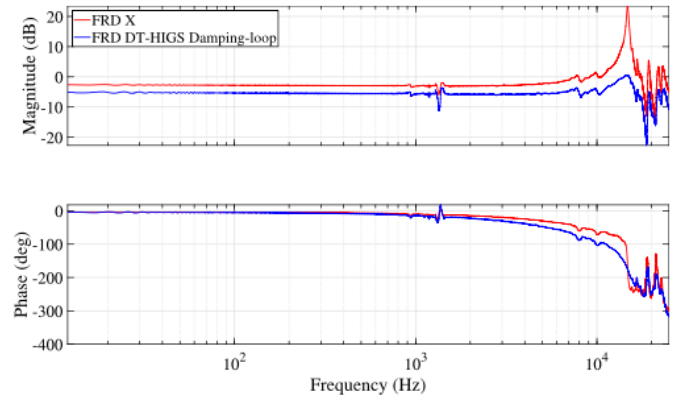


Fig. 7. Bode plot of the nanopositioning stage. With a discrete-time HIGS applied in closed loop, the nanopositioner is efficiently damped at the resonant frequency.

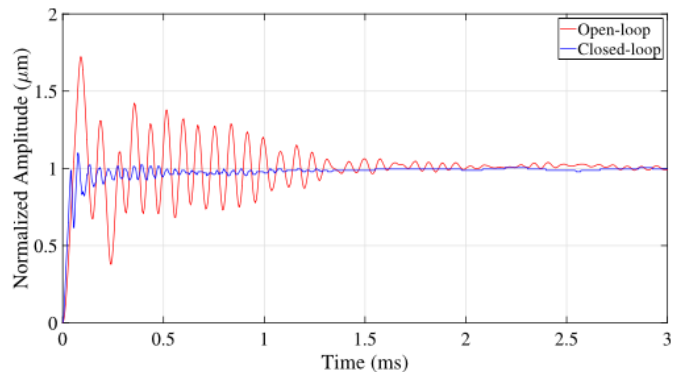


Fig. 8. Step response of the nanopositioning stage. With the discrete-time HIGS applied in the closed loop, system performance is significantly improved in terms of overshoot, rise time, and settling time.

5. Conclusion

We have proposed a control framework for the digital control of linear NI systems using discrete-time HIGS controllers. Discrete-time HIGS are shown to be SANI systems. For any linear discrete-time NI systems obtained via ZOH sampling, there exists a HIGS controller such that their closed-loop interconnection is asymptotically stable. A discrete-time HIGS asymptotically stabilizes an NI system by selecting appropriate parameters, motivating a hardware application to a high-speed flexure-guided nanopositioning system. Experimental results indicate a significant damping effect of approximately 20.4 dB at the resonance frequency.

CRediT authorship contribution statement

Kanghong Shi: Writing – review & editing, Writing – original draft, Validation, Project administration, Methodology, Investigation, Formal analysis, Conceptualization. **Erfan Khodabakhshi:** Writing – review & editing, Writing – original draft, Visualization, Validation, Software, Resources, Methodology, Investigation, Formal analysis, Data curation. **Prosanto Biswas:** Writing – original draft, Validation, Software, Data curation. **Ian R. Petersen:** Writing – review & editing, Supervision, Project administration, Funding acquisition, Conceptualization. **S. O. Reza Moheimani:** Writing – review & editing, Supervision, Resources, Project administration, Funding acquisition, Conceptualization.

Declaration of competing interest

The authors declare that they have no known competing financial interests or personal relationships that could have appeared to influence the work reported in this paper.

References

- Achten, S. P. (2020). HIGS-based skyhook damping design of a multivariable vibration isolation system.
- Angeli, D. (2006). Systems with counterclockwise input-output dynamics. *IEEE Transactions on Automatic Control*, 51(7), 1130–1143.
- Åström, K. J., & Wittenmark, B. (2013). *Computer-controlled systems: theory and design*. Courier Corporation.
- Bartolini, G. (1989). Chattering phenomena in discontinuous control systems. *International Journal of Systems Science*, 20(12), 2471–2481.
- Bhikkaji, B., Moheimani, S. O. R., & Petersen, I. R. (2011). A negative imaginary approach to modeling and control of a collocated structure. *IEEE/ASME Transactions on Mechatronics*, 17(4), 717–727.
- Bhowmick, P., & Patra, S. (2017). On LTI output strictly negative-imaginary systems. *Systems & Control Letters*, 100, 32–42.
- Brogliato, B., Lozano, R., Maschke, B., & Egeland, O. (2007). vol. 2, *Dissipative systems analysis and control: theory and applications*. London: Springer.
- Byrnes, C. I., & Lin, W. (1994). Losslessness, feedback equivalence, and the global stabilization of discrete-time nonlinear systems. *IEEE Transactions on Automatic Control*, 39(1), 83–98.
- Cai, C., & Hagen, G. (2010). Stability analysis for a string of coupled stable subsystems with negative imaginary frequency response. *IEEE Transactions on Automatic Control*, 55(8), 1958–1963.
- Chait, Y., & Hollot, C. (2002). On Horowitz's contributions to reset control. *International Journal of Robust and Nonlinear Control: IFAC-Affiliated Journal*, 12(4), 335–355.
- Chen, Y., Shi, K., Petersen, I. R., & Ratnam, E. L. (2024). A nonlinear negative-imaginary systems framework with actuator saturation for control of electrical power systems. In *2024 European control conference* (pp. 2399–2404). IEEE.
- Chen, Y., Shi, K., Petersen, I. R., & Ratnam, E. L. (2024). Unified control of voltage, frequency and angle in electrical power systems: A passivity and negative-imaginary based approach. In *2024 IEEE 63rd conference on decision and control* (pp. 5783–5788).
- Clegg, J. C. (1958). A nonlinear integrator for servomechanisms. *Transactions of the American Institute of Electrical Engineers, Part II: Applications and Industry*, 77(1), 41–42. <http://dx.doi.org/10.1109/TAI.1958.6367399>.
- Das, S. K., Pota, H. R., & Petersen, I. R. (2014). A MIMO double resonant controller design for nanopositioners. *IEEE Transactions on Nanotechnology*, 14(2), 224–237.
- Das, S. K., Pota, H. R., & Petersen, I. R. (2014). Resonant controller design for a piezoelectric tube scanner: A mixed negative-imaginary and small-gain approach. *IEEE Transactions on Control Systems Technology*, 22(5), 1899–1906.
- Das, S. K., Pota, H. R., & Petersen, I. R. (2015). Multivariable negative-imaginary controller design for damping and cross coupling reduction of nanopositioners: a reference model matching approach. *IEEE/ASME Transactions on Mechatronics*, 20(6), 3123–3134.
- Deenen, D. A., Heertjes, M. F., Heemels, W., & Nijmeijer, H. (2017). Hybrid integrator design for enhanced tracking in motion control. In *2017 American control conference* (pp. 2863–2868). IEEE.
- Deenen, D. A., Sharif, B., van den Eijnden, S., Nijmeijer, H., Heemels, M., & Heertjes, M. (2021). Projection-based integrators for improved motion control: Formalization, well-posedness and stability of hybrid integrator-gain systems. *Automatica*, 133, Article 109830.
- Van den Eijnden, S., Heertjes, M. F., Heemels, W. M., & Nijmeijer, H. (2020). Hybrid integrator-gain systems: A remedy for overshoot limitations in linear control? *IEEE Control Systems Letters*, 4(4), 1042–1047.
- Van den Eijnden, S., Heertjes, M., Nijmeijer, H., & Heemels, W. M. (2023). A small-gain approach to incremental input-to-state stability analysis of hybrid integrator-gain systems. *IEEE Control Systems Letters*.
- Ferrante, A., Lanzon, A., & Ntogramatzidis, L. (2017). Discrete-time negative imaginary systems. *Automatica*, 79, 1–10.
- Freudenberg, J., Middleton, R., & Stefanopoulou, A. (2000). A survey of inherent design limitations. 5, In *Proceedings of the 2000 American control conference. ACC (IEEE cat. no. 00CH36334)* (pp. 2987–3001). IEEE.
- Ghallab, A. G., Mabrok, M. A., & Petersen, I. R. (2018). Extending negative imaginary systems theory to nonlinear systems. In *2018 IEEE conference on decision and control* (pp. 2348–2353). IEEE.
- Halim, D., & Moheimani, S. O. R. (2001). Spatial resonant control of flexible structures-application to a piezoelectric laminate beam. *IEEE Transactions on Control Systems Technology*, 9(1), 37–53.
- Heemels, W., & Tanwani, A. (2023). Existence and completeness of solutions to extended projected dynamical systems and sector-bounded projection-based controllers. *IEEE Control Systems Letters*.
- Heertjes, M., van den Eijnden, S., & Sharif, B. (2023). An overview on hybrid integrator-gain systems with applications to wafer scanners. In *2023 IEEE international conference on mechatronics* (pp. 1–8). IEEE.
- Hitz, L., & Anderson, B. D. O. (1969). Discrete positive-real functions and their application to system stability. 116, In *Proceedings of the institution of electrical engineers* (1), (pp. 153–155). IET.
- Horowitz, I., & Rosenbaum, P. (1975). Non-linear design for cost of feedback reduction in systems with large parameter uncertainty. *International Journal of Control*, 21(6), 977–1001.
- Kalman, R. E., & Bertram, J. E. (1960). Control system analysis and design via the “second method” of Lyapunov: II-discrete-time systems. *Journal of Basic Engineering*, 82, 394–400.
- Khodabakhshi, E., Nikooienejad, N., Maroufi, M., & Moheimani, S. O. R. (2022). Design and characterization of a novel high-bandwidth flexure-guided xy nanopositioner. *IFAC-PapersOnLine*, 55(27), 271–276.
- Lanzon, A., & Petersen, I. R. (2008). Stability robustness of a feedback interconnection of systems with negative imaginary frequency response. *IEEE Transactions on Automatic Control*, 53(4), 1042–1046.
- Mabrok, M. A., Kallapur, A. G., Petersen, I. R., & Lanzon, A. (2013). Spectral conditions for negative imaginary systems with applications to nanopositioning. *IEEE/ASME Transactions on Mechatronics*, 19(3), 895–903.
- Mabrok, M. A., Kallapur, A. G., Petersen, I. R., & Lanzon, A. (2014). Generalizing negative imaginary systems theory to include free body dynamics: Control of highly resonant structures with free body motion. *IEEE Transactions on Automatic Control*, 59(10), 2692–2707.
- Middleton, R. H. (1991). Trade-offs in linear control system design. *Automatica*, 27(2), 281–292.
- Nešić, D., Teel, A. R., & Kokotović, P. V. (1999). Sufficient conditions for stabilization of sampled-data nonlinear systems via discrete-time approximations. *Systems & Control Letters*, 38(4–5), 259–270.
- Patra, S., & Lanzon, A. (2011). Stability analysis of interconnected systems with “mixed” negative-imaginary and small-gain properties. *IEEE Transactions on Automatic Control*, 56(6), 1395–1400.
- Pota, H., Moheimani, S. O. R., & Smith, M. (2002). Resonant controllers for smart structures. *Smart Materials and Structures*, 11(1), 1.
- Preumont, A. (2018). vol. 246, *Vibration control of active structures: an introduction*. Springer.
- Sharif, B., Alferink, D. W., Heertjes, M. F., Nijmeijer, H., & Heemels, W. (2022). A discrete-time approach to analysis of sampled-data hybrid integrator-gain systems. In *2022 IEEE 61st conference on decision and control* (pp. 7612–7617). IEEE.
- Shi, K., Khodabakhshi, E., Biswas, P., Petersen, I. R., & Moheimani, S. O. R. (2024). Discrete-time integral resonant control of negative imaginary systems: Application to a high-speed nanopositioner. *ArXiv Preprint:2406.16263*.
- Shi, K., Nikooienejad, N., Petersen, I. R., & Moheimani, S. O. R. (2022). A negative imaginary approach to hybrid integrator-gain system control. In *2022 IEEE 61st conference on decision and control* (pp. 1968–1973). IEEE.
- Shi, K., Nikooienejad, N., Petersen, I. R., & Moheimani, S. O. R. (2024). Negative imaginary control using hybrid integrator-gain systems: Application to MEMS nanopositioner. *IEEE Transactions on Control Systems Technology*, 32(3), 718–730.
- Shi, K., & Petersen, I. R. (2024). Digital control of negative imaginary systems: A discrete-time hybrid integrator-gain system approach. In *2024 European control conference* (pp. 2611–2616). IEEE.
- Shi, K., Petersen, I. R., & Vladimirov, I. G. (2023). Output feedback consensus for networked heterogeneous nonlinear negative-imaginary systems with free-body motion. *IEEE Transactions on Automatic Control*, 68(9), 5536–5543.
- Shi, K., Petersen, I. R., & Vladimirov, I. G. (2024). Discrete-time negative imaginary systems from ZOH sampling. *IFAC-PapersOnLine*, 58(17), 214–219.
- Shi, K., Petersen, I. R., & Vladimirov, I. G. (2024). Necessary and sufficient conditions for state feedback equivalence to negative imaginary systems. *IEEE Transactions on Automatic Control*, 69(7), 4657–4672.
- Shi, K., Vladimirov, I. G., & Petersen, I. R. (2021). Robust output feedback consensus for networked identical nonlinear negative-imaginary systems. *IFAC-PapersOnLine*, 54(9), 239–244.
- Van Den Eijnden, S. J., Heertjes, M. F., Heemels, W. M., & Nijmeijer, H. (2021). Frequency-domain tools for stability analysis of hybrid integrator-gain systems. In *2021 European control conference* (pp. 1895–1900). IEEE.
- Van Dinther, D., Sharif, B., Van den Eijnden, S., Nijmeijer, H., Heertjes, M. F., & Heemels, W. (2021). Overcoming performance limitations of linear control with hybrid integrator-gain systems. *IFAC-PapersOnLine*, 54(5), 289–294.
- Xiong, J., Petersen, I. R., & Lanzon, A. (2010). A negative imaginary lemma and the stability of interconnections of linear negative imaginary systems. *IEEE Transactions on Automatic Control*, 55(10), 2342–2347.

